Department
of
Physics

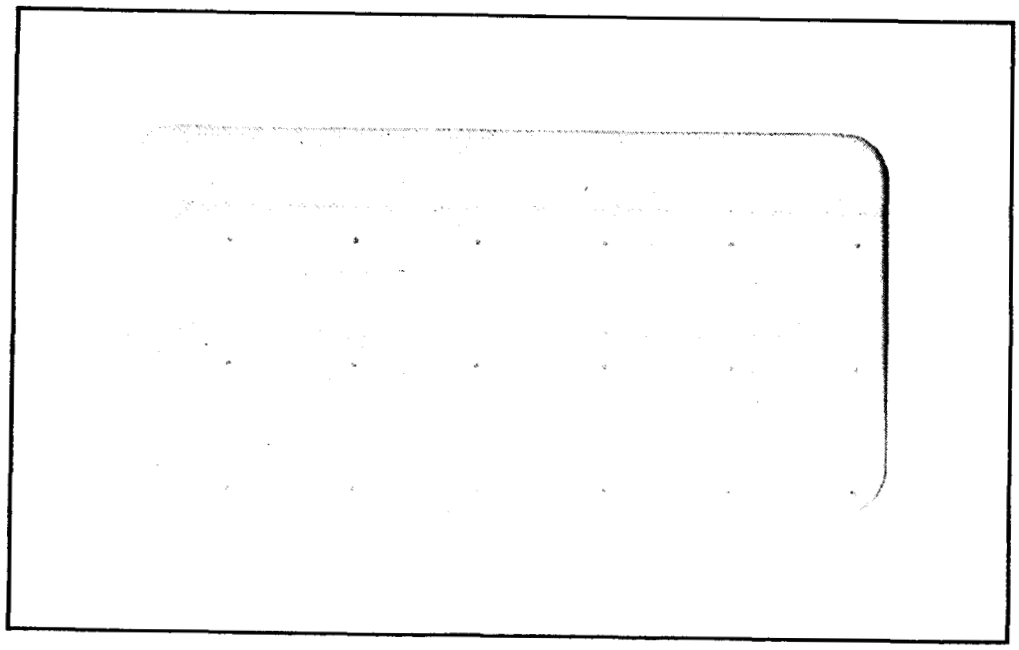

Colorado State University

Fort Collins, Colorado

RESEARCH PROJECT: Grant NSG 1594
Approaching the "Ultimate" Velocimeter: Measuring Molecular Flows With Stimulated Raman Scattering

PROJECT DURATION: 1 February 1979 - 31 August 1986

PROJECT MONITOR: Dr. R. J. Exton

PRINCIPAL INVESTIGATOR: Dr. C. Y. She
Department of Physics
Colorado State University
Fort Collins, Colorado 80523

FINAL REPORT

for

National Aeronautics and Space Administration
Langley Research Center

Coherent Raman Spectroscopy for Supersonic Flow Measurements

ABSTRACT

In collaboration with NASA/Langley Research Center, a truly nonintrusive and nonseeding method for measuring supersonic molecular flow parameters had been proposed and developed at Colorado State University. The feasibility of this Raman Doppler Velocimetry (RDV), currently operated in a scanning mode, has been demonstrated not only in a laboratory environment at Colorado State University but also in a major wind tunnel at NASA/Langley Research Center. This report summarizes the research progress of this new RDV development. In addition, methods of coherent Rayleigh-Brillouin spectroscopy and single-pulse coherent Raman spectroscopy are investigated, respectively, for measurements of high-pressure and turbulent flows.

COHERENT RAMAN SPECTROSCOPY FOR SUPERSONIC FLOW MEASUREMENTS

INTRODUCTION

Since its first report [Yeh and Cummins, 1964] laser Doppler velocimetry (LDV) for measuring fluid flows have under gone more than two decades of research, development, and applications; much progress has been made. Since the signal strength of LDV depends on scattered light intensity from naturally occurring or carefully seeded particulate matter in the flow, the accuracy of LDV is limited by the problem of particle drag making its effectiveness questionable at supersonic speeds. Spectroscopic methods that could probe the motion of atoms or molecules directly are therefore of obvious interest. Using laser-induced fluorescence with sodium or iodine seeding, speeds of mean molecular flow have been determined by measuring either the transit time [Proden et al., 1982] or Doppler shift [Miles, 1975; McDaniel et al., 1983] of the seeding atoms or molecules. The seeding requirement, however, is often unacceptable or sometimes difficult to achieve, e.g. in combustion or flame. To avoid these difficulties, we have proposed the use of coherent Raman spectroscopy for flow velocity measurements [She et al., 1981]. The Doppler shift of a fluid component, such as nitrogen molecules, is measured directly; with this method, no seeding is required whatsoever.

The feasibility of this ultimate idea, Raman Doppler Velocimetry (RDV) has soon been demonstrated in laboratory environments with

coherent anti-Stokes spectroscopy (CARS) at Stanford [Gustafson et al., 1981] and with stimulated Raman gain spectroscopy (SRGS), inverse Raman spectroscopy (IRS), and coherent Stokes Raman spectroscopy (CSRS) by our group at Colorado State University [Herring et al., 1981, 1983a; Moosmüller, 1985]. In addition, we have also demonstrated the use of IRS technique to measure temperature and pressure [Herring et al., 1983a] as well as to map out the two-component velocity distribution of a supersonic jet [Moosmüller et al., 1984]. Very recently, using a retrometer to minimize the effect of mechanical vibration and to obtain simultaneous forward and backward scattering data, the RDV has been successfully applied in a major supersonic wind tunnel at NASA/Langley Research Center providing measurements of molecular flow velocity, temperature, and pressure pertaining to a simple aerodynamic model [Exton and Hillard, 1986]. Thus, in six years, the RDV technique is becoming an ideal tool for wind tunnel measurements and for aerodynamic research at transonic and supersonic speeds.

In these current versions of RDV, two laser (pump and probe) beams, one of which is tunable, are focussed and crossed at the molecular flow of interest. As the tunable laser is scanned across the molecular resonance, the Doppler shift of Raman resonance, $\Delta\omega_D$, is measured, from which the flow velocity $\vec{v}$ is determined, by

$$\Delta\omega_D = (\vec{k}_p - \vec{k}_l)\cdot\vec{v}, \tag{1}$$

where $\vec{k}_l$ and $\vec{k}_p$ are, respectively, the wave vectors of the pump and probe laser beams. Since the kinematics of the interaction is quite general, the pump and probe method for measuring molecular flow (Eq. 1)

should not be restricted to Raman scattering only. Indeed, the use of other scattering techniques, such as those for various types of conventional laser Doppler velocimetry [She and Kelley, 1985] and a new coherent Rayleigh-Brillouin scattering method for molecular flow measurement [Herring et al., 1983b] have been established.

In this report we review the physical principles of molecular light scattering and discuss velocity, temperature, and pressure dependences in a molecular light scattering spectrum. The methods of extracting state parameters of flowing molecular gas from coherent Raman spectra as well as other types of coherent light scattering spectra will be presented and recent results reviewed. In addition, possible future developments as well as the potential and limitation of using coherent light scattering spectroscopy for molecular flow measurements will be discussed.

THEORY

To illustrate the usefulness of light scattering spectroscopy for flow measurements, it is perhaps simplest to consider a specific example. Figure 1 shows the spectrum of scattered light of simple molecules such as nitrogen. The incident laser is assumed to be monochromatic. Vibrational and rotational motions of the molecule give rise to Raman scattering:vibrational spectrum and associated rotational sidebands around 2000 cm^{-1}, and pure rotational spectrum around 100 cm^{-1}. Near the incident laser frequency, there is a low-frequency quasi-elastic scattering spectrum resulting from the translational motion of the molecules; its shape depends on the scattering geometry as well as the state of the molecular gas. The scattering geometry is

determined by the scattering wavevector $\vec{K}$ which is defined as the difference between incident and scattered wavevectors. When the scattering wavelength $\Lambda(2\pi/K)$ is smaller than the mean-free-path L, the molecular system exhibits single particle behavior; we have Rayleigh scattering with a Doppler broaden spectrum. When $\Lambda/L \gg 1$, the molecules move collectively; scattering from the Doppler shift of this collective motion leads to additional peaks at a frequency depending on its (sound) velocity; this triplet spectrum is called Rayleigh-Brillouin spectrum.

Since the location and shape of vibrational Raman, rotational Raman, and Rayleigh-Brillouin spectra depend upon pressure, temperature and velocity of the flowing molecular gas, each portion of the scattering spectrum can be used to determine these flow parameters of interest. When molecules are flowing, the peaks of vibrational Raman, rotational Raman, and Brillouin spectra, in the non-relativistic limit, will be Doppler shifted by an amount proportional to its flow (drift) velocity. Measurement of the Doppler shift provides a determination of the flow speed by each spectroscopic technique. Extensive theoretical study of Rayleigh-Brillouin scattering spectrum in the past decade [Tenti et al., 1974] has made accurate determination of pressure and temperature by Rayleigh-Brillouin scattering possible. The random collisions of molecules also gives rise to a broadening of rotational and vibrational Raman spectra whose widths depend on pressure as well as translational temperature. In addition, the Stokes/anti-Stokes intensity ratio of vibrational Raman spectra and the relative intensities of rotational sidebands can be used to determine, respectively, the vibrational and rotational temperatures of the gas. For a measurement time greater than the rotational and vibrational life

time of the gas, the system is in thermal equilibrium and the measured translational, rotational, and vibrational temperatures should be the same.

Since the spectral resolution of a spectrometer, typically 1 cm^{-1} = 30 GHz, is much too coarse for the Doppler shift of interest, <1 GHz, the methods of coherent light scattering with resolution limited only by laser linewidths must be used. In a coherent light scattering experiment, two laser beams, a pump at ω_1 and a probe at ω_p, are crossed at the molecules of interest as shown in Fig. 2(a). An exchange of energy between the two laser beams via two-photon process takes place leading to a gain or loss in the probe beam; in addition, a coherent generation (emission) of a third light beam at ω_e, via four-photon process, occurs simultaneously. If the frequency of one laser beam either ω_1 or ω_p, is tunable, their frequency difference can be made to match the characteristic frequency of the medium, Δ. Under this condition, the scattering process, said to be in resonance, is easily detectable giving rise to a peak in the measured spectrum. The characteristic (vibration or rotational) frequency of the molecule can then be determined this way. There are four types of coherent spectroscopies yielding similar spectroscopic information about the medium in question. The choices depend solely on signal-to-noise considerations as well as the availability of specific laser systems. The schematic descriptions of these processes are shown in Fig. 2(b). Both gain and loss spectroscopies are two-photon processes in which the probe beam either gains energy (with the probe at the Stokes frequency $\omega_p = \omega_s = \omega_1 - \Delta$) or loses energy (with the probe at the anti-Stokes frequency $\omega_p = \omega_a = \omega_1 + \Delta$). The emission spectroscopies are the result

of four-wave mixing processes generating a third beam at the anti-Stokes frequency $\omega_e = \omega_a = \omega_1 + \Delta$ when the probe is at ω_s or at the Stokes frequency $\omega_e = \omega_s = \omega_1 - \Delta$ when the probe is at ω_a. Although the signal of the two-photon processes is stronger than that of the four-photon processes, the signal-to-noise of these spectroscopies is in the shot-noise limit roughly the same.

In order to assess the feasibility of a given experiment, a brief discussion of signal strength is in order. The signals in question are either the change in probe power, ΔP_p, and/or the generated power of the third beam, P_e, respectively for two-photon and/or for four-photon processes. The detected signal depends on the laser powers, beam crossing angle, and for four-photon processes on the fulfillment of the phase-matching condition [Prior, 1983] as well. As the beam crossing angle decreases, signal increases at the expense of spatial resolution of the measurement. For Gaussian beams, the coherent signals near resonance may be calculated from the following formulae:

$$|\Delta P_p| = \eta_2 G(\omega_p) P_p \qquad \text{for gain or loss spectroscopy} \qquad (2)$$

$$P_e = \eta_4 (0.241) G(\omega_p)^2 P_p \qquad \text{for emission spectroscopy} \qquad (3)$$

The exact expression for P_e in terms of gain function with Gaussian beams, $G(\omega_p)$, to our knowledge, is not given in the literature. The factor 0.241 is derived from a numerical integration under the phase-matching condition for four-wave mixing interactions. The gain function G, in SI units, may be written as

$$G(\omega_p) = [4\pi^3 c\omega_1 n_1/\hbar\omega_p^3]Ng(\omega_p)(d\sigma/d\Omega)P_1 \qquad (4)$$

where n_1, N and P_1 are respectively refractive index at the pump frequency, molecular concentration and pump laser power. For Raman processes, $g(\omega_p)$ is the Raman lineshape function; it is to be replaced by $(\hbar\Delta/k_BT)S(K,\Delta)$ for Rayleigh-Brillouin processes [She et al., 1985]. The function $S(K,\Delta)$ is the spectral density function for Rayleigh-Brillouin scattering [Tenti et al., 1974]. The differential cross section $d\sigma/d\Omega$ may be obtained from spontaneous scattering measurements for both Raman and Rayleigh-Brillouin processes. The signal strength can be estimated from Eqs. (2), (3), and (4) for various cases.

The crossing efficiencies η_2 and η_4 for the two-photon and four-photon processes are functions of $x = (f/a)\tan\theta$ depending on the crossing angle θ, beam radius a, and the focal parameter f. For two completely overlapping Gaussian beams, $\eta_2 = \eta_4 = 1$. For x larger than one, these crossing efficiencies may be calculated approximately from the following formulae:

$$\eta_2 = (2/\pi)\tan^{-1}[(x^2 - 1)^{-1/2}] \qquad (5a)$$

and

$$\eta_2 = (x^2 - 1)^{-1/2} \qquad (5b)$$

where $x = (f/a)\tan\theta$. The crossing efficiencies may be calculated exactly by numerical integration by considering beam overlaps. The solid curve in Fig. 3 is a plot of the exact η_2 for $\theta = 6.5°$. Compared to Eq. (5a) shown as the dotted curve, the approximate validity of above formulae for $x > 1$ is evident.

The accuracy of any measurement depends on signal-to-noise and available measurement time. The accuracy of flow velocity measurement by coherent Raman spectroscopy when a laser source is scanned in frequency may be expressed in terms of signal-to-noise, measurement time and Raman linewidth. A practical formula for estimating measurable uncertainty in flow speed is given in the Appendix.

METHODS OF COHERENT RAMAN SPECTROSCOPY

After the initial measurement of a subsonic speed in a N_2 flow using counter-propagating stimulated Raman-gain spectroscopy [Herring et al., 1981], supersonic flow in a miniature wind tunnel was made by inverse Raman spectroscopy using two overlapping copropagating Gaussian beams. The experimental setup is shown in Fig. 4. A cylindrically symmetric converging-diverging section (made from Pyrex tubing) with a minimum throat diameter of 1.8 mm is followed by a 3.5-mm-diameter constant-area test section 3 cm in length. A N_2 bottle provides a pressure of 550 torr at the input to the wind tunnel while a 300-liter/min mechanical pump keeps the output section of the test region at about 70 torr. This arrangement produces a Mach 2 flow.

The probe laser is a 5145-Å cw single-mode Ar-ion laser. Typically, 200 mW of probe laser power is used in the measurement region. The high-power pump laser is a pulse-amplified cw dye laser; a 100 mW single-mode cw dye-laser beam is passed through three stages of amplification pumped by a frequency-doubled Nd:YAG laser operating at 10 pulses/sec. This scheme provides dye-laser pulses of 5-nsec in width, 2-MW in peak power, and with a Fourier-limited bandwidth of 100 MHz. The pump and probe beams are overlapped and directed along the

axis of the wind tunnel. Both beams are then focused with a 10-cm lens into the center of the test section. The beam confocal parameter is estimated to be 2 mm. After the interaction, the two beams are separated with a prism and filters, and the probe beam is monitored by a high-speed photodiode. To reduce the noise that is due to probe intensity fluctuations differential detection on the probe signal is employed. The pump dye laser is tuned to around 5845 Å, which corresponds to Raman resonances from the Q branch of the $v = 0$ to $v = 1$ vibration transition in N_2. As the dye laser is scanned, the IRS signal (after subtraction of the laser noise) is filtered with an RC high-pass filter, amplified, averaged by a boxcar integrator, and recorded on an x-y recorder.

To make velocity measurements, the Raman spectra from flowing N_2 and stationary N_2 are compared. From these we measure the Doppler shift and hence the velocity. Since the high-velocity and stationary spectra are not recorded simultaneously, an absolute-frequency reference is necessary to account for possible dye-laser drifts. So a small part of the dye laser beam is sent into and I_2 absorption cell, and the Doppler-free saturated-absorption spectrum of I_2 is recorded simultaneously with each IRS spectrum. This permits comparison of Raman spectra obtained at different times by simply overlapping the I_2 spectra. The many lines recorded in an I_2 spectrum correspond to hyperfine components of a single rotational-vibrational transition near 5854 Å. The results of a typical 10-min velocity measurement in the copropagating case are shown in Fig. 5. The pump and probe powers in the interaction region are 1.5 MW and 200 mW, respectively. The shift of 110 MHz in the Raman spectrum corresponds to a flow velocity of 475 m/sec. The precision of

our measurements is better than 5%. Twelve different measurements were made for the same flow conditions. This group gives an averaged Doppler shift of 109 MHz with a standard deviation of 3 MHz, corresponding to a flow velocity of 471±13 m/sec.

For the same flow, a sample temperature measurement is shown in Fig. 6, which shows two different 30-GHz scans over the lines J = 8, 9, 10. The top curve illustrates the relative intensities of these lines at room temperature, and the bottom curve shows the intensities for supersonic flow with a clear reduction in the J = 10 line, indicating expansion cooling. Since the linewidths for different J values in a given flow condition are assumed to be the same, the ratio of the heights of the J = 8 and J = 10 lines can be used to determine the gas temperature. The bottom trace gives a temperature of about 170 K. For three consecutive measurements, the maximum variation in the measured temperature is about 30 K for room-temperature measurements but is only 10 K for the 175-K measurements. The smaller absolute errors at lower temperatures are expected for a given signal-to-noise ratio.

Density measurements can also be made from the traces in Fig. 6. The density at a room-temperature, 70-torr, stationary condition can be determined from the ideal gas law. With this value, the ratio of the integrated Raman intensities is used to determine the N_2 density under the supersonic flow condition. Using data (J = 8) shown in Fig. 6, we obtain a density of about 2.2×10^{18} cm^{-3}. As with the temperature measurements, the results of three consecutive measurements on the same flow indicate uncertainties of about 10% or less. For density measurements we compare integrated intensities rather than peak heights because the linewidths (for the same J value) for different flow

conditions are expected to have different Doppler and pressure broadening. In fact, the flow velocities in our interaction region may not be uniform, which could lead to a small but detectable additional broadening. In principle, if the temperature, laser linewidth, and this additional (velocity) broadening are known, the Raman linewidths can be used to measure the pressure of the supersonic flow directly.

Using a retrometer system and overlapping Gaussian beams, Exton and Hillard were able to obtain both copropagating (forward) and counter-propagating (backward) inverse Raman spectra of the molecular flow in the same frequency scan. Such a combined spectrum is schematically shown in Fig. 7. The difference between forward and backward Doppler shifts, W, may be related to the velocity component along the beams,

$$W = (\Delta\omega_D)_B - (\Delta\omega_D)_F = 2\omega_p(v/c)\cos\varphi \qquad (6)$$

where v is the magnitude of the velocity vector, φ the angle between the (colinear) laser beams and the velocity vector, and ω_p is the probe frequency. Since the pressure broadening contributes to linewidth equally in both forward and backward geometry, while Doppler broading (temperature dependent) contributes much less in the forward scattering, the measurement of both forward and backward linewidths allows a determination of both pressure and temperature of the flowing gas. A chart showing the temperature and pressure dependencies of forward and backward linewidths is shown in Fig. 8. Using this unified approach, Exton and Hillard have been able to measure distributions of molecular flow velocity, static pressure and translational temperature in a supersonic wind tunnel in both free-stream operation and near a simple

aerodynamic model [Exton and Hillard, 1986] demonstrating the feasibility of RDV for wind tunnel applications.

If two probe beams with proper crossing angles to the pump beam are used, two velocity components of a flow can be measured simultaneously [Moosmüller et al., 1984]. To determine two perpendicular velocity components we have to make $(\vec{k}_1 - \vec{k}_a)$ and $(\vec{k}_1 - \vec{k}_a')$ perpendicular to each other. For a given Raman shift Δ and probe-laser wavelength λ_a, this leads to a unique geometry for the wave vectors, as shown in Fig. 9 for $\Delta = 2330\ cm^{-1}$ and $\lambda_a = 514.5$ nm. As can be seen in this figure, it is possible to measure directly two perpendicular velocity components by crossing the two probe beams with an angle of only 6.5° to the pump beam. The spatial resolution is determined by the minimum spot size and the crossing angle. In our case, a spot size of 35 μm and a crossing angle of 6.5° results in an interaction length of 0.7 mm, which corresponds to an interaction volume of $0.003\ mm^3$. The smaller interaction length also results in a smaller signal compared with the colinear arrangements. In our case the signal is reduced by roughly a factor of 30.

The experimental set up is shown in Fig. 10. The supersonic jet is generated by expanding N_2 from a back pressure of 9.8 bars through a nozzle with a diameter D of 1.51 mm into a background pressure of 53 mbars. A N_2 bottle provides gas with sufficient pressure, and the background pressure is maintained by a 4300-liter/min mechanical pump. Using an empirical formula [Ashkenas and Sherman, 1966], we determine the length of the supersonic region to be 13.7 mm. The pump and probe beams are as described before and they are focused by lenses with 20-cm

focal length. At their foci the probe beams intersect symmetrically the focus of the pump beam at an angle of 6.5°.

To make velocity measurements, Raman spectra of stationary and flowing N_2 have to be compared. Initially we attempted to record the spectrum of stationary N_2 in a copropagating-beam arrangement simultaneously with the spectrum of flowing N_2, which is taken in a crossed-beam arrangement. Comparing spectra of stationary N_2 with both arrangements, we observed a systematic frequency shift on the order of 100 MHz. This shift is possibly due to a Stark effect and will be investigated further in the future. To avoid this complication, we have taken reference spectra of stationary N_2 with the setup used for the flow measurement. To account for a possible frequency drift of the dye laser between the different scans, we use part of the cw dye-laser beam to record a saturated absorption spectrum simultaneously in I_2. The hyperfine components of an I_2 line are then used as an absolute-frequency reference. The result of a typical 10-min measurement of two velocity components on the axis of the jet is shown in Fig. 11. Both peaks are shifted nearly symmetrically relative to the peak of a spectrum of stationary N_2. This indicates a flow velocity perpendicular to the pump beam, as expected. We have mapped out the velocity distribution of a center plane of the jet sequentially. The results of these measurements are shown in Fig. 12, along with the boundary of the supersonic jet determined from a simple Schlieren setup. The velocity vectors behave in general as expected. We observe expansion and acceleration with increasing distance from the nozzle exit. We have also investigated the temperature distribution within the jet.

Because of the need to frequency scan one laser beam to obtain the desired Raman spectrum for determining the Doppler shift, a velocity measurement as described above typically requires between 5 to 10 min. Although the relatively long measurement time of the current RDV is acceptable in certain wind tunnel applications, it is a severe limitation for tunnels with short run-time or tunnels under turbulent flow conditions. This fact has been recognized even in our initial proposal [She et al., 1981] which contains some suggestions to reduce the measurement time. More recently, the possibility for velocity measurement with single-pulse coherent Raman spectroscopy has been re-examined [She, 1983]; it concluded that with the development of a specialized probe laser and high-resolution spectrum analyzer, single-pulse flow velocity measurements should be possible. Very recently we have conceived yet another method for performing single-pulse velocity measurement with coherent Raman spectroscopy [She, 1987]. We suggested the use of a narrow-band pulse pump laser together with a cw probe laser consisting of several discrete frequency components separated by an amount smaller than the Raman linewidth of interest. In this case, a discrete spectrum of coherent line emissions (CARS or CSRS), one associated with each probe frequency component, can be detected. Analysis of this discrete spectrum by a suitable interferometer should allow the determination of the spectral peak, Doppler shift and hence the flow velocity. The advantage of this new technique over the other single-pulse methods lie in the fact that the required probe laser can be implemented from a cw single-frequency laser by the method of electro-optic (either amplitude or frequency) modulation. With the successful implementation of any single-pulse measurement method, the

RDV technique should become a truly noninvasive, real-time probe for aerodynamic research under any flow conditions imaginable, laminar or turbulent.

As described in the Appendix, the accuracy of velocity determination is limited by the available signal-to-noise in an experiment. With current scanning method, the nominal speed uncertainty is around 1 m/sec; the uncertainty is expected to increase for the proposed single-pulse measurement for lack of averaging. In principle, with higher pump power the coherent Raman signal can be made to increase. However, the presence of optical Stark effect, as pointed out previously, will be a fundamental limit that cannot be ignored. Since Stark shift which is about 0.1 cm^{-1} per 1 TW/cm^2 [Rahn et. al., 1980] depends only on intensity, higher pump power may be used in a life-size wind tunnel without over penalizing spatial resolution. Optical Stark effect is of interest in its own right in nonlinear optics; its continued study is in progress.

COHERENT RAYLEIGH-BRILLOUIN TECHNIQUE

As mentioned in the Introduction, both Raman and fluorescence techniques are good spectroscopic methods for measuring molecular flows; however, they have a common problem. The pressure broadening of the Q-branch ($v = 0 \rightarrow v = 1$) Raman transition in molecular nitrogen is 2.4 GHz/atm. This broadened linewidth makes the determination of the Doppler shift more difficult and the technique less sensitive for velocity measurements at higher pressures. The pressure effect on fluorescence is even more destructive. In addition to line broadening, the fluorescence of iodine and sodium is quenched by one order of

magnitude at a nitrogen pressure of 0.1 atm. Thus these spectroscopic techniques for velocity measurements are becoming increasingly impractical at pressures exceeding 1 atm. Although most wind tunnels use pressures lower than 1 atm, there are important large facilities that are operated at higher pressures. An outstanding example is the new NASA National Transonic Facility, which typically operates at a flow from Mach 0.2 to 1.2 and a nitrogen pressure between 1 and 9 atm. For velocity measurements of such high-pressure flows, a different spectroscopic technique is apparently needed. We now discuss the use of stimulated Rayleigh-Brillouin-gain spectroscopy for measuring atomic- or molecular-flow velocities. This technique is most suitable for flows with a pressure greater than 1 atm because,unlike the Raman or fluorescence techniques, its sensitivity improves as the gas pressure increases.

Rayleigh-Brillouin-gain spectroscopy is a form of coherent scattering spectroscopy in which the frequencies of the probe, ω_1, and pump, ω_2, lasers, one of which is tunable, are within a few GHz of each other. Similarly to stimulated Raman scattering, the Rayleigh-Brillouin spectrum shows gain on the stokes side ($\omega_2 > \omega_1$) and loss on the anti-Stokes side ($\omega_2 < \omega_1$), leasing to a zero crossing at $\omega_1 = \omega_2$. Figure 13 shows the qualitative difference of stimulated Rayleigh-Brillouin-gain spectra of nitrogen at 0.9 and 4.1 atm. The fact that the signal-to-noise ratio of the 4.1-atm spectrum is much better and its width narrower is evident. Since the peak gain increases quadratically at high pressure because of the narrowing of Brillouin linewidth as the pressure increases, the method of stimulated Rayleigh-Brillouin-gain spectroscopy works better for higher pressures.

Similarly to the Raman technique, the flow velocity v may be determined from the measured Doppler shift

$$\Delta\omega_D = (\vec{k}_1 - \vec{k}_2)\cdot\vec{v} \tag{7}$$

where k_2 and k_1 are, respectively, the wave vectors of the pump and probe lasers. In addition to the flow velocity, fitting the Rayleigh-Brillouin-gain spectrum to a theoretical model can yield a determination of the local values of thermal conductivity, viscosity, temperature, and gas density.

The experimental setup is shown in Fig. 14. The probe laser is a single-mode cw dye laser (1-MHz linewidth), and the pump laser consists of an identical cw dye laser along with a three-stage pulsed amplifier (peak power 1 MW, 5-nsec pulses, 10 pulses/sec, and 150-MHz linewidth). The two counterpropagating laser beams were crossed at an angle of 1° and focused with 20-cm lenses to a waist of approximately 25 μm and an interaction length of 3 mm. The flow from a converging nozzle was directed at an angle of 15° with respect to the crossed laser beams. This measurement was made in the turbulent subsonic region (after the normal shock) about 3 cm downstream from the nozzle. The 1-mm-diameter nozzle was backed with 5.69×10^3 torr of nitrogen and exhausted into room air. After it had traversed the interaction region, the probe beam was monitored with a high-speed photodiode followed by a high-pass filter and an amplifier. The signal was then averaged by a boxcar integrator. As the pump laser is frequency scanned across the probe-laser frequency, a stimulated Rayleigh-Brillouin-gain spectrum is recorded. The gain spectra with flows directed in opposite directions and with stationary

air are compared, and the Doppler shifts that are due to the flow are determined. The result for flow-velocity measurements using stimulated Rayleigh-Brillouin-gain spectroscopy is shown in Fig. 15, where spectra of flow directed along the pump and probe beams are shown. The spectrum of stationary room air (not shown), which has a comparable signal-to-noise ratio, would fall between the Rayleigh-Brillouin spectra, if superimposed. An iodine fluorescence spectrum was recorded simultaneously with each Rayleigh-Brillouin-gain spectrum for a frequency reference. The shift between peaks (or zero crossing) is determined to be 1.2 GHz, corresponding to a relative velocity of 350 m/sec. The gain spectra were repeated three times for each direction, yielding nine different measurements of the same flow. These measurements had a maximum discrepancy of 60 m/sec. Since this discrepancy is independent of the flow velocity, the percentage measurement uncertainty would be smaller for faster flows.

The technique is obviously applicable to supersonic flows. Although the measurements reported here are done at atmospheric pressure, the Rayleigh-Brillouin signal should increase drastically with gas pressure. Flow-velocity measurements and the determination of other local flow parameters (viscosity, temperature, and density) at pressures higher than 1 atm can be made nonintrusively with lasers using stimulated Rayleigh-Brillouin-gain spectroscopy. Other advantages in Rayleigh-Brillouin spectroscopy for flow measurements include the facts that the same laser system may be used for any molecular system and that, unlike vibrational Raman scattering, it works for atomic systems as well. Like coherent Raman spectroscopy, other forms of coherent

Rayleigh-Brillouin spectroscopies at different crossing angles can also be used to probe atomic and molecular flows.

CONCLUSION

In this report, we have presented a unified discussion of coherent light scattering spectroscopy and its application for a nonintrusive determination of the state of flowing molecular gas. These include measurements of flow velocity, gas temperature and static pressure. The feasibility of using coherent Raman spectroscopy for this purpose has been demonstrated not only in the laboratory but also in a major wind tunnel. The advantage of using coherent Rayleigh-Brillouin scattering for measuring high pressure flow is discussed and its feasibility demonstrated in the laboratory. In addition, the possibility and methods of single-pulse flow measurements is discussed; its successful implementation will make the RDV method a truly nonintrusive real-time probe in aerodynamic research for measuring any flow imaginable, laminar or turbulent.

REFERENCES

Askhenas, H. and Sherman, F. S., in "4th International Symposium on Rarefied Gas Dynamics," J. H. DeLeeuw, ed. (Academic, New York, 1966), Vol. 2, p. 84.

Exton, R. J. and Hillard, M. E., "Raman Doppler velocimetry: a unified approach for measuring molecular flow velocity, temperature and pressure," Appl. Opt. 25, 14 (1986).

Gustafson, E. K., McDaniel, J. C., and Byer, R. L., "CARS measurement of velocity in a supersonic jet," IEEE J. Quant. Electr. QE-17, 2258 (1981).

Herring, G. C., Fairbank, Jr., W. M., and She, C. Y., "Observation and measurement of molecular flow using stimulated Raman gain spectroscopy," IEEE J. Quant. Electr. QE-17, 1975 (1981).

Herring, G. C., Lee, S. A., and She, C. Y., "Measurement of a supersonic velocity in a nitrogen flow using inverse Raman spectroscopy," Opt. Lett. 8, 214 (1983a).

Herring, G. C., Moosmüller, H., Lee, S. A., and She, C. Y., "Flow velocity measurements with stimulated Rayleigh-Brillouin-gain spectroscopy," Opt. Lett. 8, 602 (1983b).

McDaniel, J. C., Hiller, B., and Hanson, R. K., "Simultaneous multi-point velocity measurements using laser-induced iodine fluorescence," Opt. Lett. 8, 51 (1983).

Miles, R. B., "Resonant Doppler Velocimeter," Phys. Fluids 18, 751 (1975).

Moosmüller, H., Herring, G. C., and She, C. Y., "Two-component velocity measurements in a supersonic nitrogen jet with spatially resolved inverse Raman spectroscopy," Opt. Lett. 9, 536 (1984).

Moosmüller, H., private communication (1985).

Prior, Y., "Three-dimensional phase matching in four-wave mixing," Appl. Opt. 19, 1741 (1980).

Prodan, J. V., She, C. Y., and Fairbank, Jr., W. M., "An atomic fluorescence transit-time velocimeter," Opt. Commun. 43, 215 (1982).

Rahn, L. A., Farrow, R. L., Koszykowski, M. L., and Mattern, P. L., "Observation of an optical Stark effect on vibrational and rotational transitions," Phys. Rev. Lett. 45, 620 (1980).

She, C. Y., Fairbank, Jr., W. M., and Exton, R. J., "Measuring molecular flow with high-resolution stimulated Raman spectroscopy," IEEE J. Quant. Electr. QE-17, 2 (1981).

She, C. Y., "Proposal for measuring molecular velocity vector with single-pulse coherent Raman spectroscopy," Appl. Phys. B 32, 49 (1983).

She, C. Y., and Kelley, R. F., "Photon-burst correlation techniques for atmospheric crosswind measurements," Appl. Physics B 33, 195 (1984).

She, C. Y., Herring, G. C., Moosmüller, H., and Lee, S.A., "Stimulated Rayleigh-Brillouin gain spectroscopy," Phys. Rev. 31, 3733 (1985).

She, C. Y., "Single-pulse Raman Doppler velocimetry with an FM or AM cw probe laser beam," submitted to Appl. Opt. (1985).

Tenti, G., Boley, C.D., and Desai, R. C., "On the kinetic model description of Rayleigh-Brillouin scattering from molecular gases," Can. J. Phys. 52, 285 (1974).

Yeh, Y., and Cummins, H. Z., "Localized fluid flow measurements with a HeNe laser spectrometer," Appl. Phys. Lett. 4, 176 (1964).

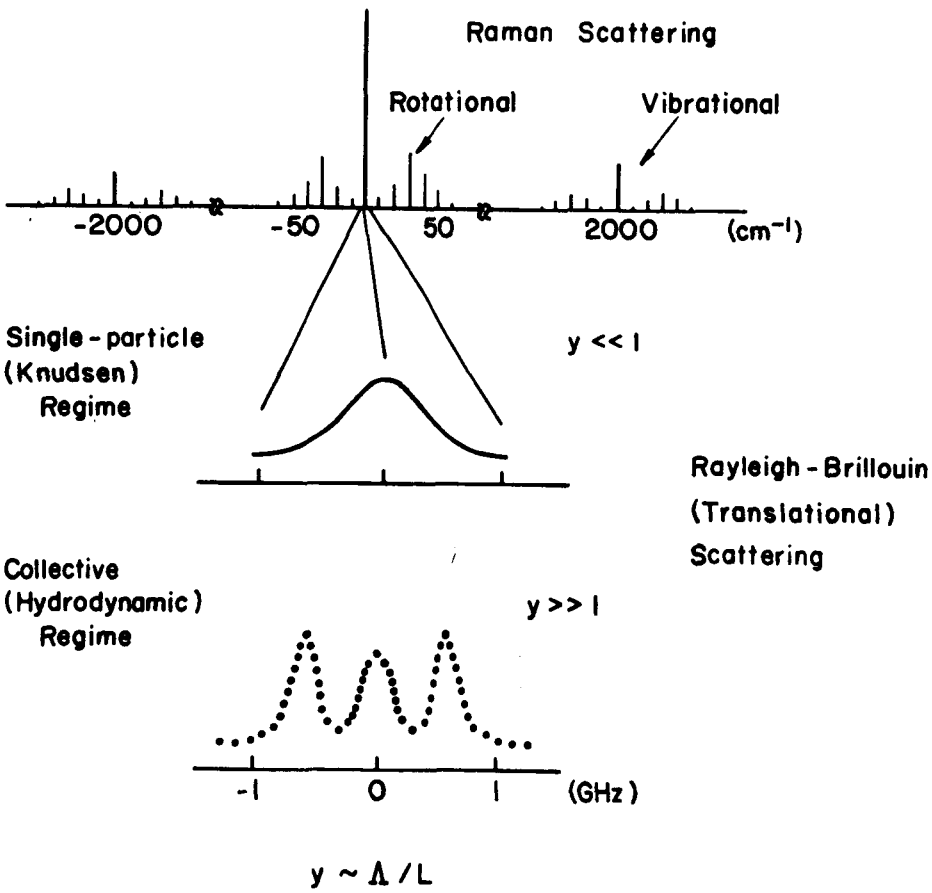

Fig. 1. Light scattering spectrum of diatomic molecule, e.g. nitrogen.

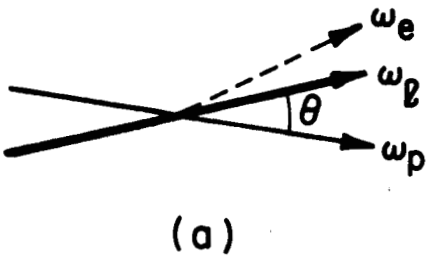

(a)

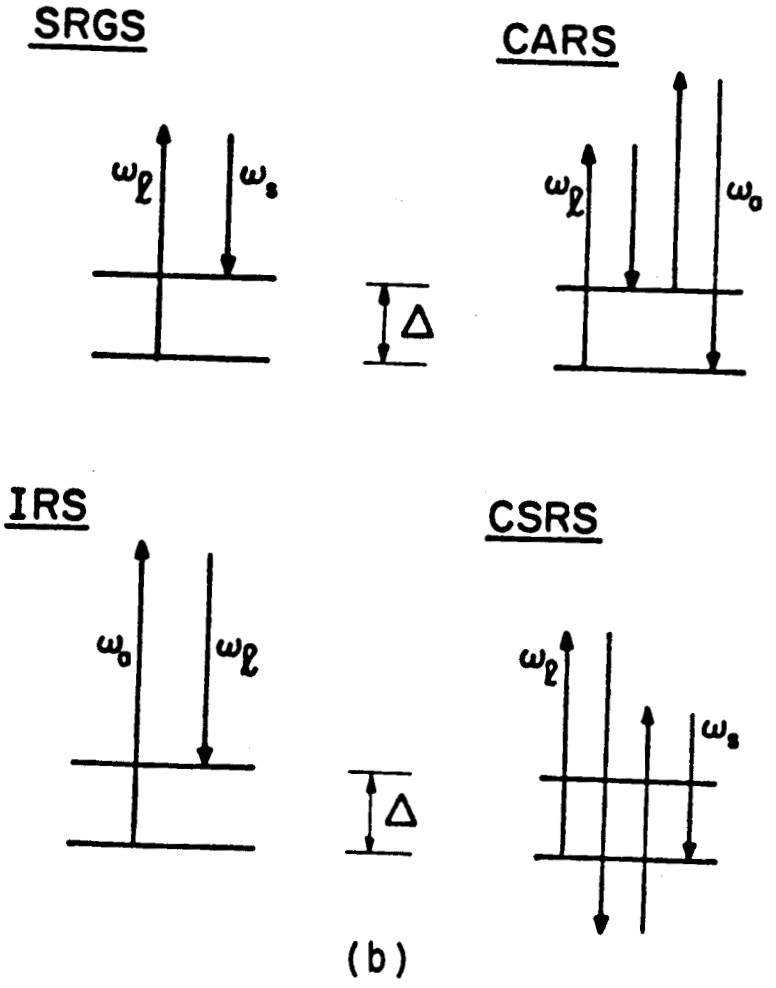

(b)

Fig. 2. Coherent Raman processes: (a) pump and probe beams crossing at an angle θ. (b) energy diagram describing four types of processes.

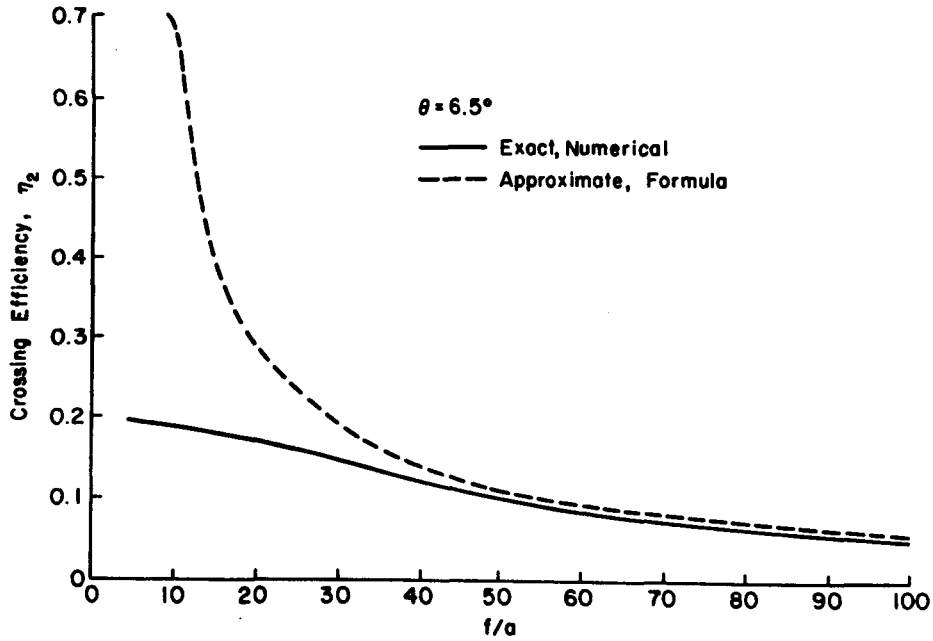

Fig. 3. Crossing efficiency of the two-photon process as a function of f/a (θ = 6.5°).

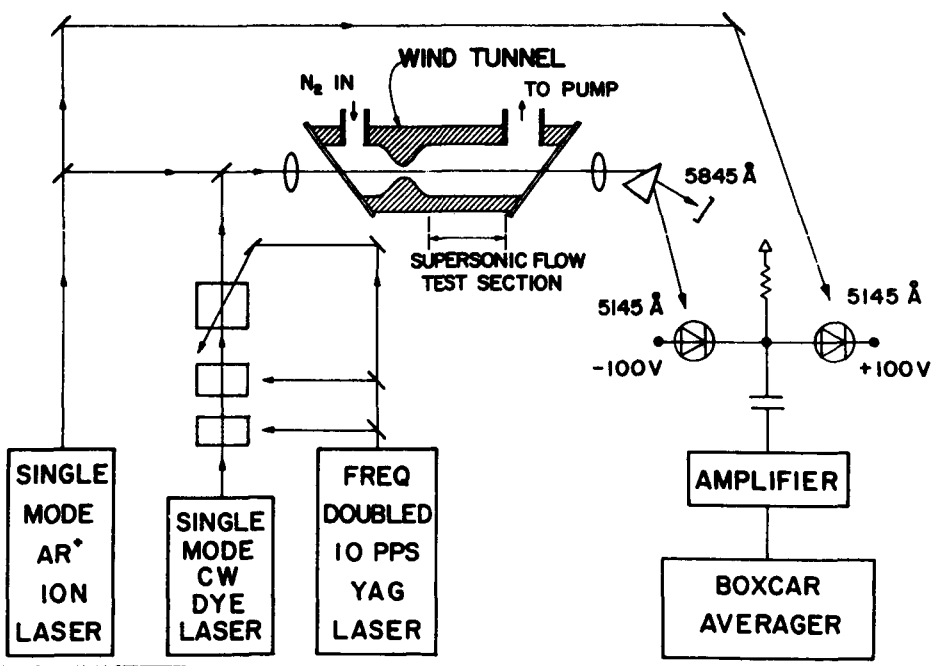

Fig. 4. Experimental setup for inverse Raman spectroscopy using copropagating geometry. [Following Herring et al., 1983a.]

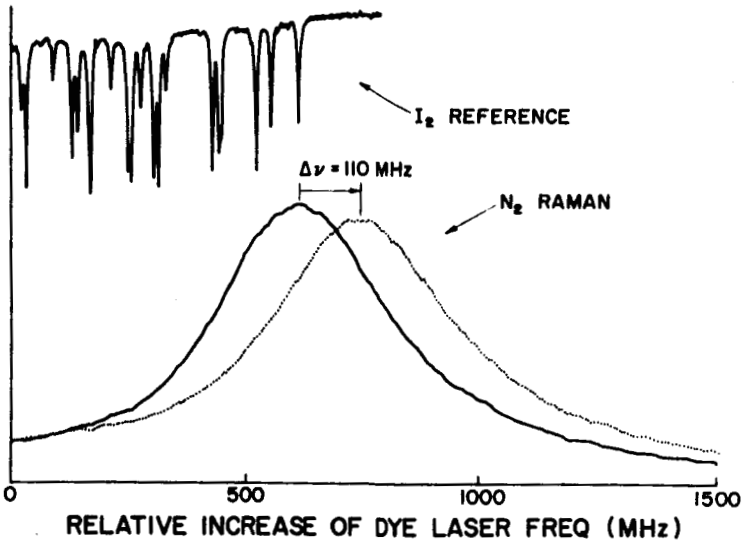

Fig. 5. Sample copropagating frequency shift of J = 8 for a 475 m/sec flow. [Following Herring et al., 1983a.]

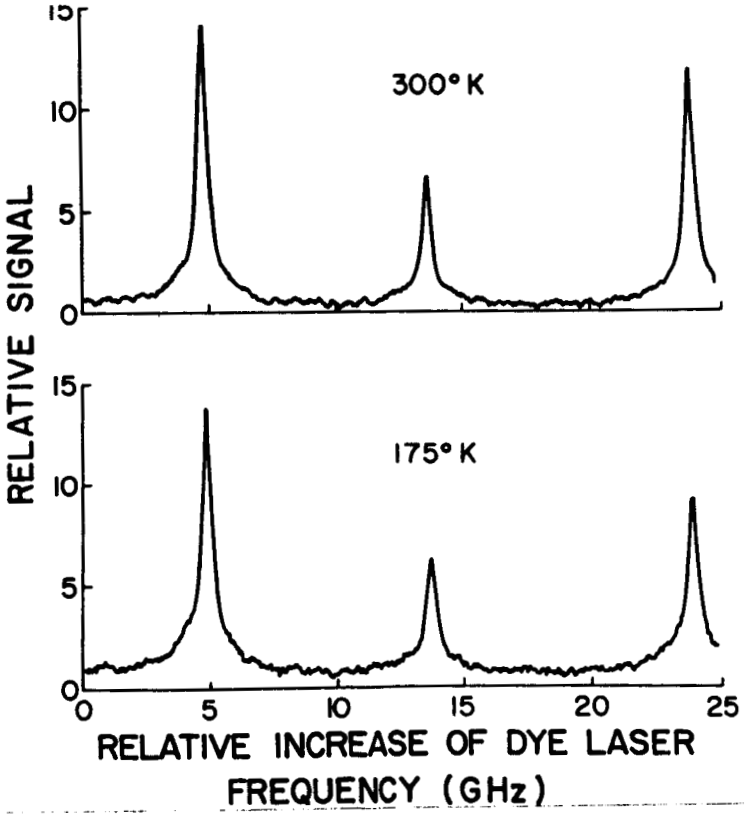

Fig. 6. Sample temperature measurements showing the relative intensities of J = 10 (right-most peak). [Following Herring et al., 1983a.]

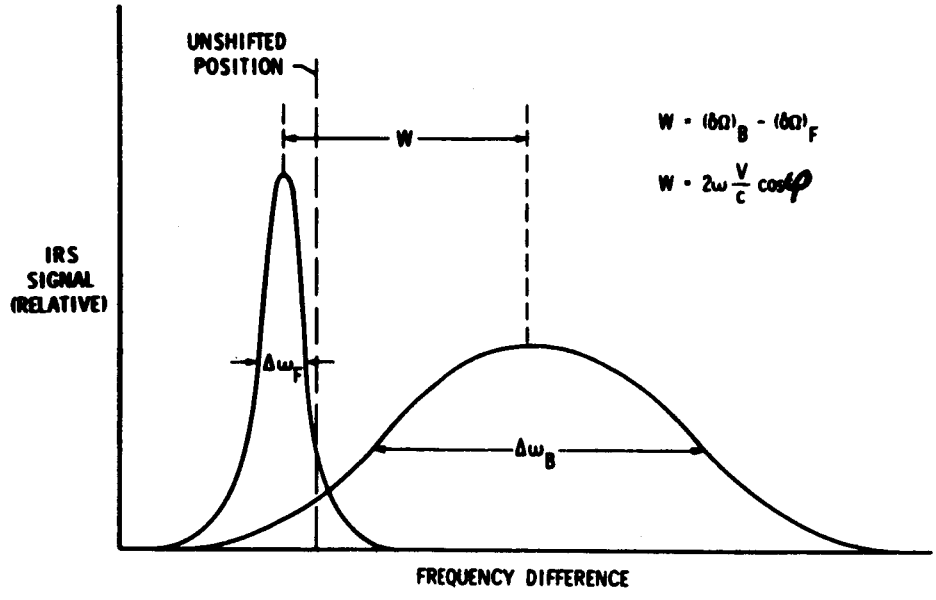

Fig. 7. Sketch of the shift and breadth of the forward and backward scattered Raman lines relative to the unshifted (zero velocity) position. [Following Exton and Hillard, 1986.]

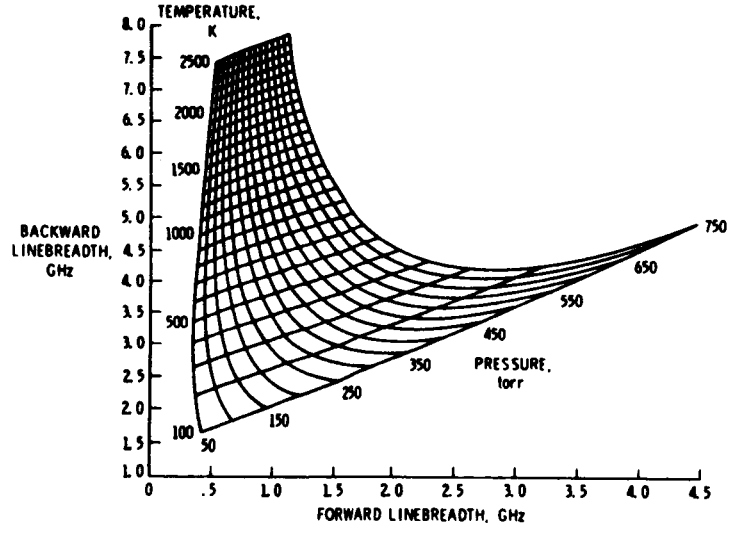

Fig. 8. Backward and forward Voight line breadths (FWHM) are shown for the N_2 Q-branch (J = 10) line over a wide range of temperature and pressure. [Following Exton and Hillard, 1986.]

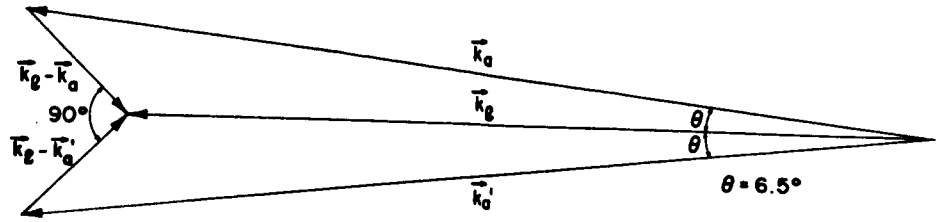

Fig. 9. Geometry of the wave vectors for pump beam ($\vec{k}_1$) and probe beams ($\vec{k}_a$, $\vec{k}_a$). [Following Moosmüller et al., 1984.]

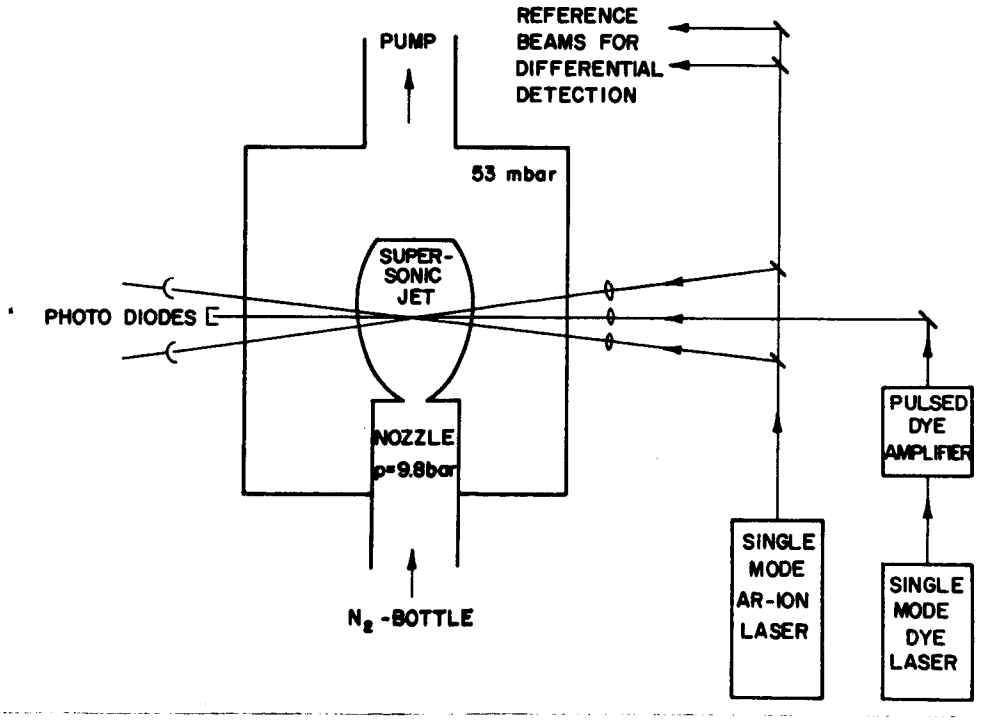

Fig. 10. Experimental setup for the measurement of two perpendicular velocity components with IRS. [Following Moosmüller et al., 1984.]

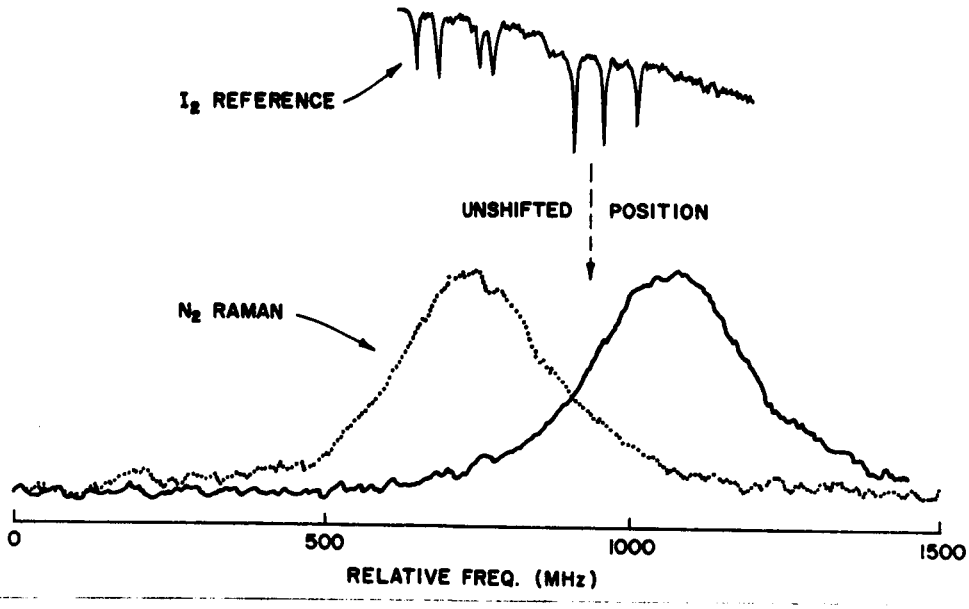

Fig. 11. Stimulated Raman spectra of the Q-branch (J – 4) of N_2. The shifts of the two peaks correspond to two velocity components. [Following Moosüller et al., 1984.]

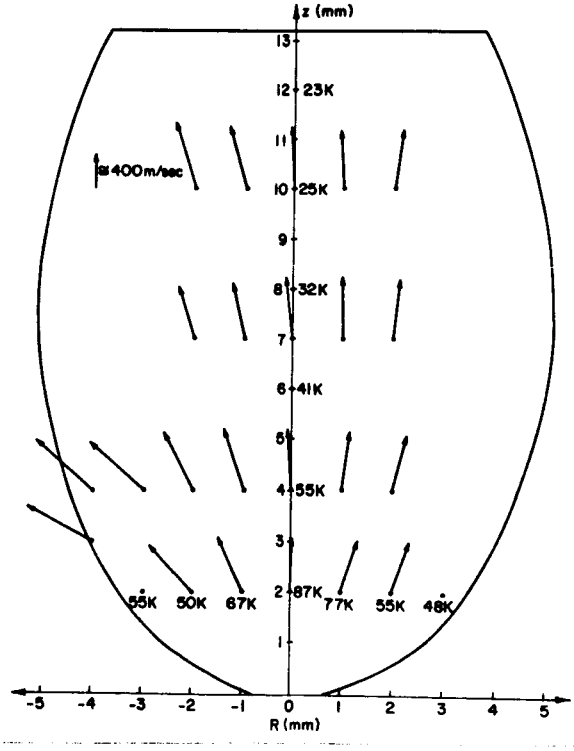

Fig. 12. Flow-velocity and temperature distribution in the supersonic jet. [Following Moosmüller et al., 1984.]

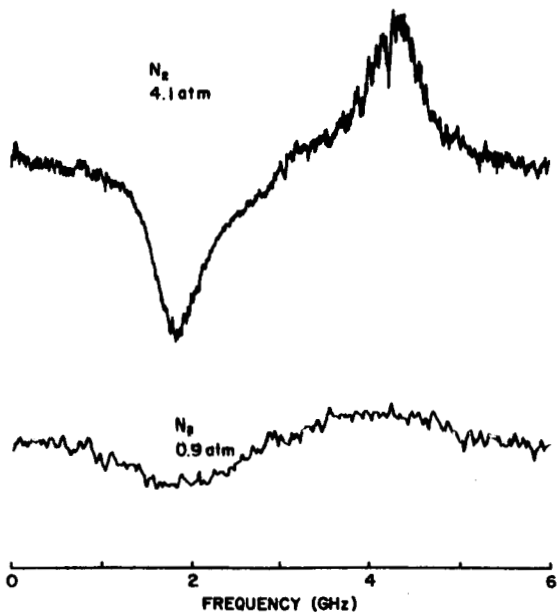

Fig. 13. Typical stimulated Rayleigh-Brillouin-gain spectra of nitrogen at 0.9 and 4.1 atm. [Following Herring et al., 1983b.]

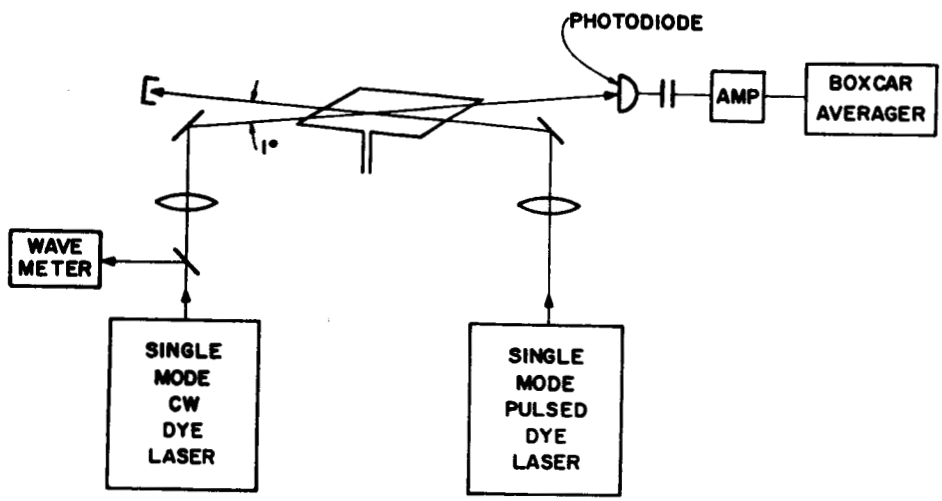

Fig. 14. Experimental setup for flow velocity measurements with stimulated Rayleigh-Brillouin-gain spectroscopy. [Following Herring et al., 1983b.]

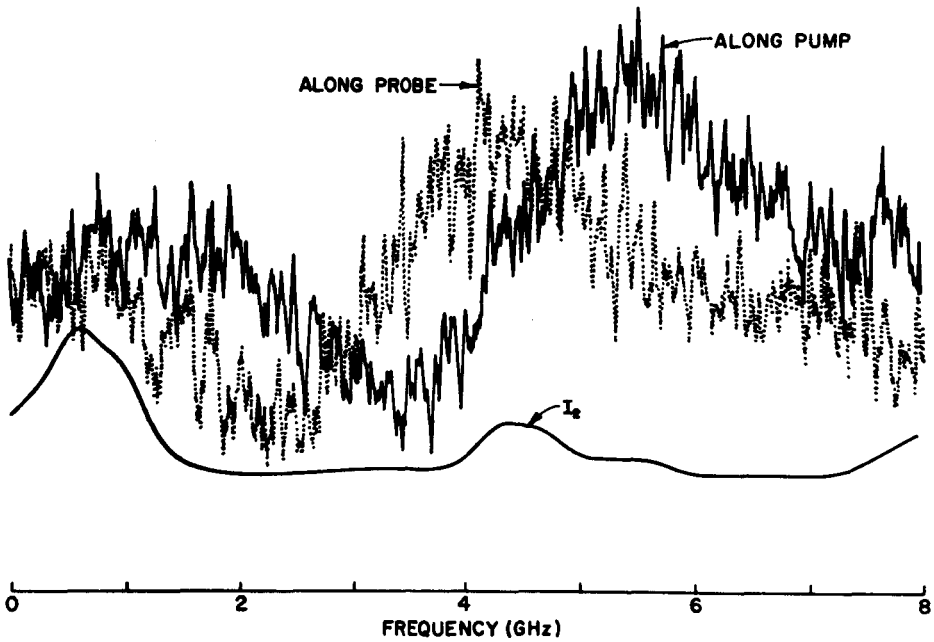

Fig. 15. Typical result of flow-velocity measurements. The obvious shift between the peaks of these Rayleigh-Brillouin-gain spectra corresponds to a relative velocity of 350 m/sec. [Following Herring et al., 1983b.]

APPENDIX

Uncertainty in Spectral Peak Determination

In looking for a new spectroscopic feature or carrying out a precision measurement with tunable lasers, one is concerned with the availability of adequate signal-to-noise for the experiment. Once proceeding with the experiment, one simply uses as much measurement time as needed to achieve the best possible relative accuracy and, if necessary, by repeating the measurement many times. The absolute accuracy of the experiment is usually limited by the availability of a standard reference, nearby in frequency, for comparison. In applied spectroscopy, one usually deals with a known feature whose spectrum has been well characterized under a given environment, e.g. temperature, pressure, etc. Probing a slight change or shift of the spectroscopic feature is used as a tool to determine the experimental condition in question. Because a dynamic change is of interest the time, with which a spectroscopic measurement is made, is thus limited. In this case the relative measurement accuracy depends on available measurement time as well as signal-to-noise ratio (S/N). Since the changes are being measured, the absolute accuracy in frequency is usually not an issue.

The dependence of measurement accuracy on S/N and measurement time is derived and discussed in this Appendix. Although only coherent Raman spectroscopy and the associated achievable accuracy for the flow velocity measurement will be considered, the analysis should have general validity for any type of spectroscopy when a laser source is scanned in frequency. Since a pulsed laser is used, the signal is detected at a repetition rate r with an integration time constant t by a

box car integrator. Each detection interval Δt, which is set by the pulse width or box car window, is determined by the transform-limited bandwidth of the detection system. Along with these quantities, the signal-to-noise in a detection interval, S/N, which depends on laser power and its intensity fluctuation, ∂, and the measurement time, T, are the only parameters input to the analysis. The aim of the analysis is to provide a working guide for estimating the achievable accuracy of an anticipated measurement,not to give a statistical treatment of the measurement. Thus, the result of the analysis is useful but not absolute; it is subjected to the interpretation of detection bandwidth, $1/\Delta t$, and integration time constant, t.

For coherent Raman spectroscopy, the signal-to-noise in a detection interval is well known. It is given, respectively for SRGS (IRS) and CARS (CSRS) as

$$S/N = \frac{G}{[\partial^2 + 2\hbar\omega_s/QP_s\Delta t]^{1/2}} \quad \text{and} \quad S/N = \frac{G}{[G^2\partial^2 + 2\hbar\omega_a/Q\eta P_s\Delta t]^{1/2}}$$

where G, $\hbar$, ω_s, ω_a, Q, P, and η are, respectively, Raman gain, Planck constant, Stokes frequency,anti-stokes frequency, detector quantum efficiency, probe power, and a reduction factor of the CARS (CSRS) process which is due to mismatch of optical phases and beam profiles. The laser intensity fluctuation, ∂, is the fractional uncertainty of the probe laser for the SRGS (IRS) process and of twice of the pump plus that of the probe laser for the CARS (CSRS) process. It is worthwhile to note that in the shot-noise limit SRGS and CARS have comparable S/N. However, if the experiment is limited by laser intensity fluctuation

noise, CARS has more favorable S/N unless the stimulated Raman gain, G, is nearly unity. In an integration time constant t, there are n (=rt) detection intervals averaged to give a signal-to-noise of the measurement,

$$S/N = (S/N)\sqrt{n} = (S/N)\sqrt{(rt)} \qquad (A1)$$

For simplicity, a symmetric bell-shape spectrum is assumed. The uncertainty in determining the spectral peak obviously depends on S/N of the measured spectrum. More Specifically, the following Gaussian and Lorenzian spectra are considered:

$$y = y_0 \exp[-(\nu - \nu_0)^2/2\beta^2] \quad \text{and} \quad y = y_0/[(\nu - \nu_0)^2 + \beta^2]$$

For both these spectra, the maximum spectral change occurs at $\nu - \nu_0 = \pm\beta$, where the spectrum is reduced from the peak by 0.50 and 0.61, respectively, for Gaussian and Lorenzian profiles. Here, the uncertainty in measurable frequency, $\Delta\omega$, may be related to the fractional spectral uncertainty as

$$dy/d\nu = y/\beta \quad \text{or} \quad \Delta\nu = (dy/y)\beta = \beta/(S/N) \qquad (A2)$$

One may locate the spectral peak by locating the points with maximum slope and then declare their midpoint as the peak. For all intents and purposes, the points with maximum slope may be regarded as the half-power points. The S/N in Eq. (A1) refers to the signal-to-noise at these frequencies. The optimum situation is to scan the laser at a

rate, R, which covers the minimum resolvable spectrum $\Delta\nu$ in an integration time constant, t, i.e. $R = \Delta\nu/t$. The adequate measurement time is somewhat arbitrary, although it is quite reasonable to set $T = 4\beta/R$. These conditions together with Eqs. (A1) and (A2) yield the measurement uncertainty and integration time constant; they may be expressed in terms of repetition rate r, measurement time T, and signal-to-noise S/N as

$$\Delta\nu = (4/rT)^{1/3}\beta(S/N)^{-2/3} \quad \text{and} \quad t = (4S/N)^{-2/3}T^{2/3}r^{-1/3} \qquad (A3)$$

Equation (A3) is the main result of the present analysis. For example, consider an experiment with the gain at the half-power point $G = 0.05$, $T = 300$ sec, $\beta = 250$ MHz, $r = 10$, $Q = 0.1$, $\omega_s = 5 \cdot 10^{14}$ Hz, $\Delta t = 10^{-8}$ sec, and $P_s = 50$ mW in the shot-noise limit. For the peak rotational line ($J = 8$) in the Q-branch nitrogen Raman spectrum, this requires a pump power less than 0.5 MW. The calculated values are $S/N = 434$, $\Delta\omega = 0.48$ MHz, and $t = 0.14$ sec. If the experiment is limited by laser intensity noise, S/N is much smaller, e.g. 10. In this case, one calculates $\Delta\nu = 6.13$ MHz and $t = 1.78$ sec. The measured signal-to-noise of the spectrum for these cases should be, respectively, $S/N = 514$ and 42. The latter value has been experimentally achieved routinely.

For a given accuracy in $\Delta\nu$, the measurable uncertainty in flow speed depends on the geometry of the experiment. If the Raman line is pressure broadened, the linewidth β remains constant and independent of the experimental geometry. The accuracy in speed measurement would be

$$\Delta v = 2\pi\Delta\nu/\Delta k, \text{ where } \Delta k = |\vec{k}_l - \vec{k}_s| \qquad (A4)$$

Continuing on the above examples, the extreme values for Δk are approximately $1.5 \cdot 10^6$ m^{-1} (copropagating geometry) and $2.0 \cdot 10^7$ m^{-1} (counter-propagating geometry). In the shot-noise limit, these correspond to a speed accuracy of 2 m/sec and 0.15 m/sec. For the laser-noise limited case, the measurable accuracies in velocity are 26 m/sec and 2 m/sec. If the spectrum is partially Doppler broadened, the linewidth should be wider for the counter-propagating geometry, and the uncertainty in velocity should be correspondingly worse than the values 0.15 m/sec and 2 m/sec given above for the counter-propagating geometry. In any case, with the pump power less than 1 MW, pump and probe beams overlapping, one may expect a typical velocity uncertainty within 1 m/sec in the shot-noise limit and 15 m/sec with laser intensity noise.

In the interest of spatial resolution, the probe and pump beams may be made to cross at an angle. This may decrease the Raman gain by a factor up to 10 or even 100. Because of the -2/3 power dependence of $\Delta\nu$ on S/N, the uncertainty in measurable frequency and velocity increases only by a factor up to 5 or 22 correspondingly. Even in the laser-noise limited case, these frequency uncertainties are still much less than the Raman linewidth, suggesting the validity of the measurement technique in the crossed geometry as well. Furthermore, this analysis remains valid for the three-component velocity measurements provided three times probe power (150 mW for the above example) is used. Although a pulsed pump laser with a repetition rate r was considered, Eq. (A3) is also valid for continuous-wave scanning laser spectroscopy if r is replaced by

$1/\Delta t$. In this case, phase-sensitive detection method with the modulated signal contained in the frequency band $1/\Delta t$, should be used.